# The Bandwidth of Helical Antennas*

T. S. M. MACLEAN† AND R. G. KOUYOUMJIAN‡

*Summary*—**The propagation along a finite helix is examined by using a propagation constant which was determined by Sensiper for the infinite helix. By utilizing the Hansen and Woodyard condition, the bandwidth variation with the dimensions of the helix is obtained. It is shown that for a pitch angle $\psi$ equal to 13°, the normally accepted bandwidth of $0.77 < C_\lambda < 1.25$, where $C_\lambda$ is the circumference in terms of free-space wavelengths, is applicable only to antennas up to about two wavelengths long. A curve showing the bandwidth as a function of length has been computed, and the shape of this curve has been confirmed experimentally. Good patterns and axial ratio with sidelobe levels no greater than −10 db were obtained for helices as long as 10 wavelengths. Good patterns and axial ratio may also be obtained for $\psi$ as small as 2° provided that the helix is sufficiently long to establish the surface wave.**

## Introduction

THE discovery of axial radiation from a uniform helix by Kraus[1] in 1947 resulted in a thorough and fairly complete investigation of the helical antenna, from the viewpoint of both pattern and impedance, over a wide frequency range. This investigation covered antennas of between three and ten turns and pitch angles of 5° to 24°. At the same time, sufficient analysis was carried out to give an adequate understanding of the operation of the antenna in terms of inward- and outward-traveling waves along the conductor. These investigations were completed by 1950.

An alternative and more complete theoretical approach to the problem of electromagnetic wave propagation along helical conductors was given by Senisper[2] in 1951, but since he was interested primarily in its application to traveling-wave tubes, and his approach was necessarily mathematical, little effort has been made to apply his results to the helical antenna. The object of the present investigation was to carry this out, and as a result, new information is available about the limits of the helical pitch angle which may be employed, and about the bandwidth of helical antennas as long as ten wavelengths.

## Phase Velocity

The characteristics of the helical antenna are functions of 1) the over-all length in free-space wavelengths ($L_\lambda$); 2) the pitch angle ($\psi$); 3) the circumference of the imaginary cylinder on which the helix is wound ($C_\lambda$); and 4) to a lesser extent, of the conductor diameter ($d_\lambda$). It is desirable to consider a single parameter, the phase velocity $v$ along the conductor, rather than each of these separately, since $v$ is a function of each of these variables and is directly related to the radiation characteristics of the helical antenna. The same simplification can also be used profitably in the case of the Yagi antenna.[3]

The determinantal equation to be solved for obtaining numerical values of phase velocity along an infinite helix is[2]

$$0 \simeq \sum_m \left\{ \left( \beta_0^2 a^2 - k^2 a^2 + k^2 a^2 \frac{m^2 \cot^2 \psi}{(\gamma_m a)^2} \right) I_m(\gamma_m a) K_m(\gamma_m a) + k^2 a^2 \cot^2 \psi I_m'(\gamma_m a) K_m'(\gamma_m a) \right\} \frac{\sin m\pi \dfrac{\delta}{h}}{m\pi \dfrac{\delta}{h}} \tag{1}$$

where

$\beta_0$ is the propagation constant to be determined,
$a$ = radius of imaginary cylinder on which the helix is wound,
$k = \omega\sqrt{\mu\epsilon}$ the free-space phase constant,
$\psi$ = helical pitch angle = $\tan^{-1} h/2\pi a$,
$\gamma_m^2 = (\beta_m^2 - k^2)$,
$\beta_m = \beta_0 + m(2\pi/h)$,
$\delta$ = tape width of helix conductor.

The primes on the modified Bessel functions denote differentiation with respect to the argument.

An alternative but essentially similar form of the equation has been given by Chodorow and Chu,[4] and it is this form which has been used in the computations throughout:

$$0 \simeq U_0 + V_0 + L_0 \sin\psi \frac{1}{\left(\frac{\delta}{h} 2\pi\right)^2} \left[ C_3(0) - C_3\left(\frac{\delta}{h} 2\pi\right) \right] + \sum_1^\infty \left[ \frac{\sin\left(m \frac{\delta}{h} \pi\right)}{\left(m \frac{\delta}{h} \pi\right)} \right]^2 \cdot \left( Y_m + Y_{-m} - L_0 \frac{\sin\psi}{m} \right) \tag{2}$$

* The research reported in this paper was sponsored in part by the U. S. Army Signal Engrg. Lab., Fort Monmouth, N. J.

† Antenna Lab., The Ohio State University, Columbus, Ohio. On leave of absence from Edinburgh University, Edinburgh, Scotland.

‡ Antenna Lab., The Ohio State University, Columbus, Ohio.

[1] J. D. Kraus, "Helical beam antenna," *Electronics*, vol. 20, pp. 109–111; April, 1947.

[2] S. Sensiper, "Electromagnetic Wave Propagation on Helical Conductors," Res. Lab. of Electronics, Mass. Inst. Tech., Cambridge, Tech. Rept. No. 194; May, 1951.

[3] H. W. Ehrenspeck and H. Poehler, "A New Method for Obtaining Maximum Gain from Yagi Antennas," presented at the WESCON Convention, Los Angeles, Calif.; August, 1956.

[4] M. Chodorow and E. L. Chu, "Cross Wound Helices for Traveling-Wave Tubes," Microwave Lab., Stanford University, Stanford, Calif., Rept. No. 249; November, 1954. Prepared under Office of Naval Res. Contract N6 onr 25123 (NR373 361).

where

$$U_0 = (\gamma_0 a)^2 K_0(\gamma_0 a) I_0(\gamma_0 a) \sin^2 \psi,$$
$$V_0 = -(ka)^2 K_1(\gamma_0 a) I_1(\gamma_0 a) \cos^2 \psi,$$
$$L_0 = (\gamma_0 a)^2 \sin^2 \psi - (ka)^2 \cos^2 \psi,$$

with

$$\gamma_m^2 = \beta_m^2 - k^2,$$
$$\beta_m = \beta_0 + m\frac{2\pi}{h},$$

$$C_3\left(\frac{\delta}{h}2\pi\right) = \sum_{m=1}^{\infty} \frac{\cos m\left(\frac{\delta}{h}2\pi\right)}{m^3}$$
$$= 1.202 + \frac{1}{2}\left(\frac{\delta}{h}\cdot 2\pi\right)^2 \log\left(\frac{\delta}{h}\cdot 2\pi\right) - \frac{3}{4}\left(\frac{\delta}{h}2\pi\right)^2 - \frac{1}{288}\left(\frac{\delta}{h}\cdot 2\pi\right)^4 - \cdots$$

$$Y_m = (\gamma_m a)^2 K_m(\gamma_m a) I_m(\gamma_m a) \sin^2 \psi + \left[\left(\frac{m\beta_m a}{\gamma_m a}\right)^2 K_m(\gamma_m a) I_m(\gamma_m a) + (ka)^2 K_m'(\gamma_m a) I_m'(\gamma_m a)\right] \cos^2 \psi - (m\beta_m a) K_m(\gamma_m a) I_m(\gamma_m a) \sin^2 \psi.$$

It is to be noted that in common with other periodic structures,[5] there are certain forbidden regions associated with the helix, in which a solution to the above equations may not be found. The regions where solutions may be found correspond to

$$\gamma_m a = [(\beta_m^2 - k^2)a^2]^{1/2} > 0 \qquad (3)$$

or

$$|\beta_m a| > ka.$$

For both positive and negative $\beta_0$ and $|m| \geq 1$, this condition becomes[2]

$$|m| + \frac{ka}{\cot\psi} < \frac{|\beta_0| a}{\cot\psi} < |m| - \frac{ka}{\cot\psi}. \qquad (4)$$

A graph of this inequality is shown in Fig. 1, where the shaded areas indicate the forbidden regions for different values of $m$. The pass band region for the beam-mode type of helical antenna is also shown. It will be noted that the forbidden regions become continuous for $ka/\cot\psi > 0.5$, *i.e.*, for $d > \lambda/2$. This condition also arises in the theory of linear end-fire arrays, where for $d > \lambda/2$ there is no longer a single major lobe in the pattern.

The choice of coordinates shown in Fig. 1 has the advantage of making the graph applicable to any value of pitch angle $\psi$, which would not be true for the $\omega-\beta$ coordinates more commonly used with periodic structures.[5] At the same time, the slope of the solution to the determinantal equation for a given value of $ka$, *i.e.*,

$$\frac{ka}{\cot\psi} \Big/ \frac{\beta_0 a}{\cot\psi},$$

still gives the axial phase velocity along the helix as it does when the $\omega-\beta$ coordinates are used.

## The Bandwidth of a Medium-Pitch Helix

The reason for obtaining numerical values of the propagation constant along an infinite helix was to determine if such values would be of use in predicting an upper frequency limit for a finite helical antenna. It is known, for example, that if the propagation constant along the conductor satisfies the Hansen-Woodyard condition along the axis, the pattern will be an optimum one for a uniform helix. If the phase velocity exceeds that for the Hansen-Woodyard condition, the width of the main lobe will be increased, while if it is lower, the sidelobe level will be increased. In order to examine the bandwidth of the medium-pitch helix quantitatively, the case of $\psi = 13°$ will be considered.

The reasons for choosing $\psi = 13°$ were that a) accurate experimental values of phase velocity for this pitch angle and for a specific length of 1.6 λ were available, and b) it was known that an angle of about this size gives the largest bandwidth for a helix 1.6 wavelengths long.

Fig. 2 illustrates this graphically for an array of 50 isotropic elements. The array factor is

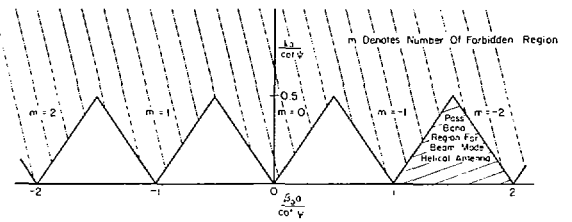


Fig. 1—Chart of forbidden regions.

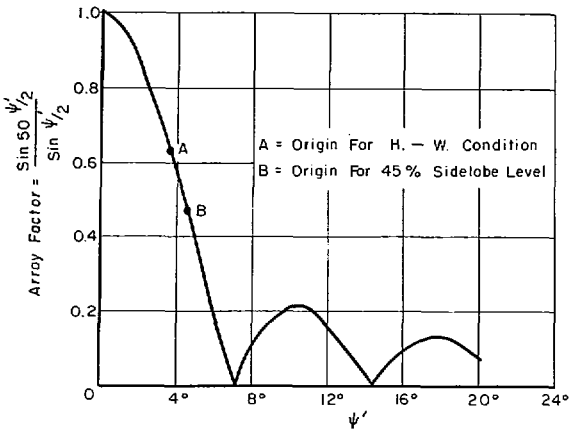


Fig. 2—Array factor for 50 isotropic elements.

[5] D. A. Watkins, "Topics in Electromagnetic Theory," John Wiley and Sons, Inc., New York, N. Y.; 1958.

$$\frac{\sin 50\psi'/2}{\sin \psi'/2},$$

where

$$\psi' = \beta d \cos\phi - \alpha$$

$$= 2\pi C_\lambda \tan\psi \cdot \cos\phi - \frac{L_\lambda}{v/c} \cdot 2\pi. \tag{5}$$

Only the part of this pattern to the right of the point corresponding to $\phi = 0°$ is traced out; this point is a function of the phase velocity $v$ along the conductor. It should be noted that $\lambda$ is the free-space wavelength. Point $A$ represents the point $\phi = 0°$ for the Hansen-Woodyard phase condition, and point $B$ is the point $\phi = 0°$ where the sidelobe level has increased to 45 per cent of the main beam. This sidelobe level will be arbitrarily taken to represent the upper allowable frequency of operation for the antenna.

It will be noted that in moving from $A$ to $B$, $\psi'$ has increased from 3.6° ($=\pi/50$) to 4.6° ($=0.080$ radian). Substituting these values in (5) and taking $C_\lambda = 1.0$ enable the two corresponding values of $v$ to be calculated. The percentage change in $v$ as $A$ moves along the array factor curve to $B$ is only 0.22 per cent. Use will be made of this result later.

Conversely, if $v$ as a function of $C_\lambda$ is known accurately, the value of $C_\lambda$ for which the sidelobe level will be equal to any percentage of the main beam can be calculated from the same equation.

In solving the determinantal equation, the normal range of $ka$ ($= C_\lambda$) from 0.7 to 1.3 has been used. Values of the phase velocity over this range are shown in Fig. 3, where it must be remembered that it is the phase velocity along the conductor which is plotted. This is related to the fundamental axial phase velocity by

$$v_{\text{conductor}} = \frac{v_{\text{axial}}}{\sin\psi}.$$

Superimposed on the same graph is the Hansen-Woodyard condition for an infinitely long array, which also represents the in-phase field condition for a finite array. It is noteworthy that over the region $0.7 < ka < 1.0$ the two curves coincide within the thickness of the curve, although (a) is always slightly below (b). This result encourages one to utilize the solution for the infinite helix in connection with the helical-antenna problem.

However, in order to estimate the upper frequency limit of the finite helix, the Sensiper solution must be compared with the Hansen-Woodyard curve for the finite helix. Fig. 4 compares the Sensiper solution with the Hansen-Woodyard condition for 50 turns. Using the point where the divergence of the two curves becomes significant, an estimate for the upper frequency limit is that $C_\lambda \approx 1.1$. This can be evaluated more accurately using (5); *i.e.*,

$$2\pi\left(C_\lambda \tan\psi - \frac{L_\lambda}{v/c}\right) = -(2\pi + 0.080).$$

It is noted that $L_\lambda = C_\lambda \sec\psi$, so that for $\psi = 13°$ there are two unknowns, $C_\lambda$ and $v$. Using the relationship between $v$ and $C_\lambda$ resulting from Sensiper's solution, the desired solution of (5) is obtained. For the case considered here the solution is $C_\lambda = 1.10$, confirming the previous estimate of the same value.

This result has been obtained by use of only the array factor for 50 turns, and the calculated phase velocity for the infinite helix. In the same way, using the array factors for 3, 5, 10, 15, $\cdots$, 45 turns, and the phase velocity for the infinite helix, the upper frequency limit $C_\lambda$ can be computed for each of these numbers of turns. The results of these computations are shown in Fig. 5 as curve (a). For comparison, the experimental results for $3 \leq n \leq 50$ turns are shown as curve (b).

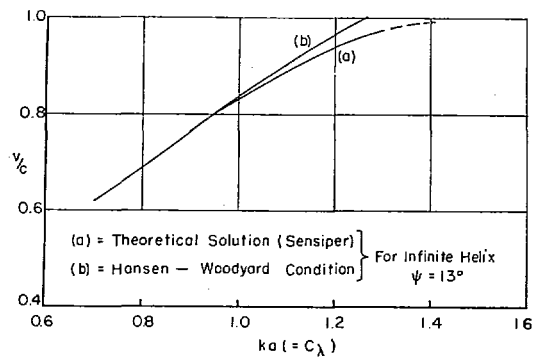


Fig. 3—Phase velocity vs circumference in wavelengths.

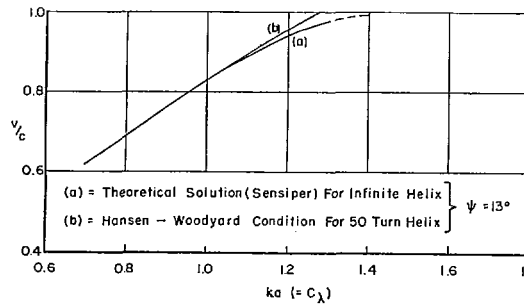


Fig. 4—Phase velocity vs circumference in wavelengths.

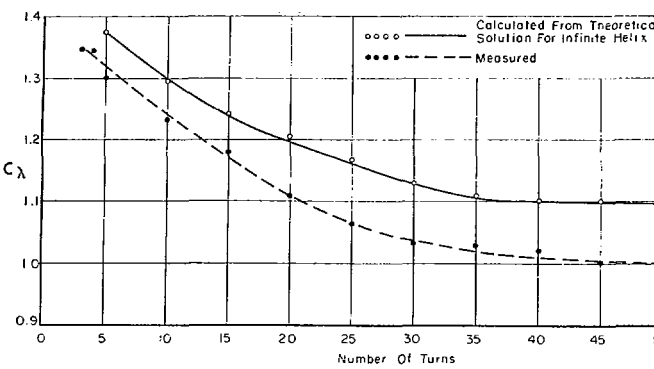


Fig. 5—Upper frequency limit vs number of turns for $\psi = 13°$.

The agreement in the variation with number of turns is satisfying, although the calculated absolute values are necessarily high. This follows since the phase velocities used correspond to those for the infinite helix, which are known to be greater than the ones applying to a finite helix.

In order to complete the picture of the variation of bandwidth with the length of the antenna, it is necessary to consider also the variation, if any, of the lower frequency limit. The physics of the situation in this case is quite different from the limitation at the upper end. There the pattern break-up is caused by the phase velocity's not increasing rapidly enough with frequency, but at the lower end the pattern begins to become useful only with the effective launching of a new transmission mode. For a 13° pitch angle, this occurs at 0.77 $C_\lambda$ for an infinite helix. Measured values of approximately 0.75 $C_\lambda$ for helices as short as 0.7 wavelength suggest that this frequency remains substantially constant with length. Therefore, in Fig. 5 it is suggested that the ordinate of upper frequency limit essentially determines the ratio of upper to lower frequency limits with a scale conversion factor of 1/0.77 or 1.3. This result corrects the earlier, quite widely held notion that the useful frequency range of a helical antenna centers in the frequency $C_\lambda = 1.0$. According to the results reported here, however, it should rather be considered as existing above $C_\lambda = 0.77$ for the 13° pitch angle case. The value of 0.77 is a fixed lower limit, while the upper limit is variable.

In obtaining the experimental results for Fig. 5(b), it was necessary to take patterns of $E_\theta$, $E_\phi$, and axial ratio for $3 \leq n \leq 50$ turns. A selection of these patterns is shown in Figs. 6–20. The most important of these are the ones for large $n$, since it is believed that these represent the patterns of the longest helices which have as yet been tested. In all cases it can be seen that both the patterns and the axial ratios are good. The measurement frequency of 8 kmc corresponds to 0.92 $C_\lambda$.

The variation of half-power beamwidth with length of the antenna is shown in Fig. 21 for the $E_\theta$ and $E_\phi$ patterns. These curves are based on the experimental measurements shown in the previous figures, and agree closely with the values which may be predicted from Hansen-Woodyard conditions. The constant frequency to which the curves are applicable is 0.92 $C_\lambda$.

At still higher frequencies corresponding to the upper bandwidth limit, the larger sidelobes are accompanied by a smaller half-power beamwidth which is plotted in Fig. 22. This occurs as the result of a reduction in phase velocity so that the array factor is shifted further into the imaginary region.[6]

In Figs. 23 and 24 the measured variation of axial ratio with length of the antenna is shown for the frequencies used in Figs. 21 and 22.

[6] F. K. Goward, "An improvement in end-fire arrays," *J. IEE*, vol. 94, pt. III, pp. 415–418; November, 1947.

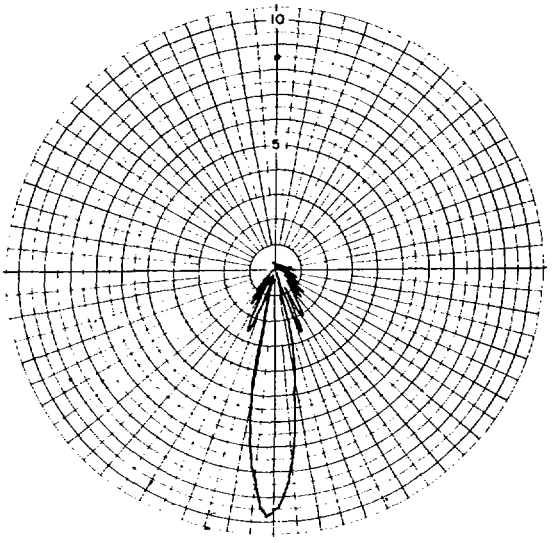


Fig. 6—$E_\theta$ pattern for 50-turn, 13° helix; $f = 8$ kmc.

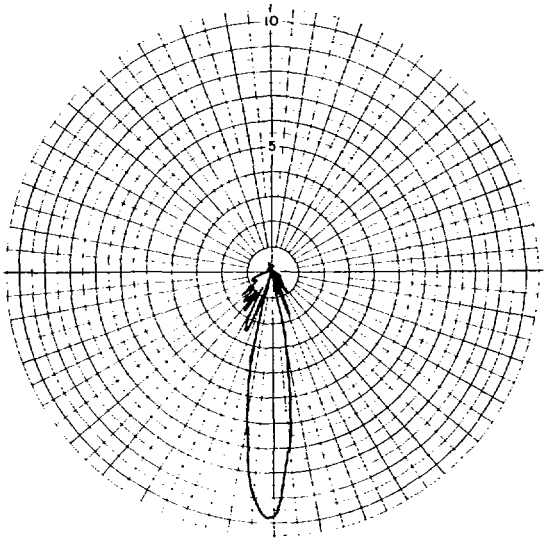


Fig. 7—$E_\phi$ pattern for 50-turn, 13° helix; $f = 8$ kmc.

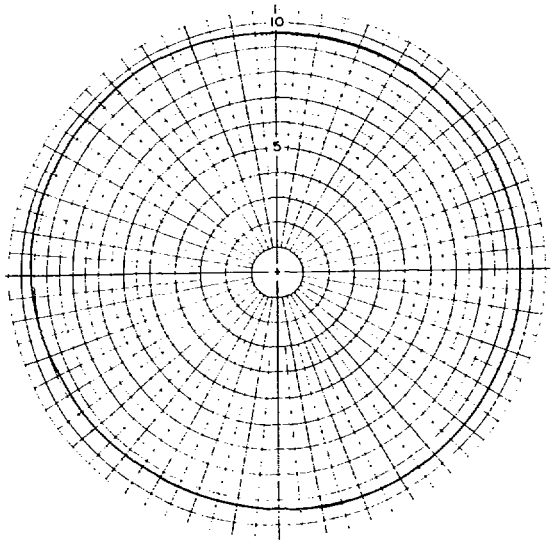


Fig. 8—Polarization pattern for 50-turn, 13° helix; $f = 8$ kmc.

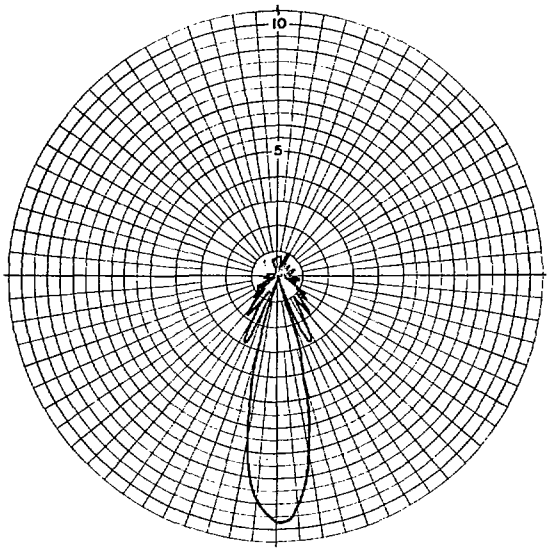


Fig. 9—$E_\theta$ pattern for 40-turn, 13° helix; $f=8$ kmc.

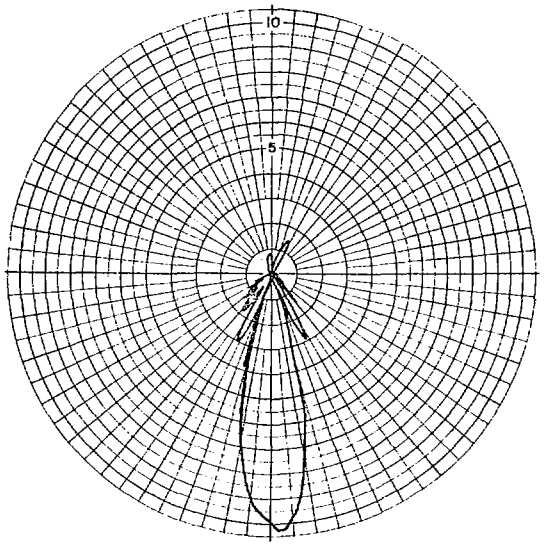


Fig. 10—$E_\phi$ pattern for 40-turn, 13° helix; $f=8$ kmc.

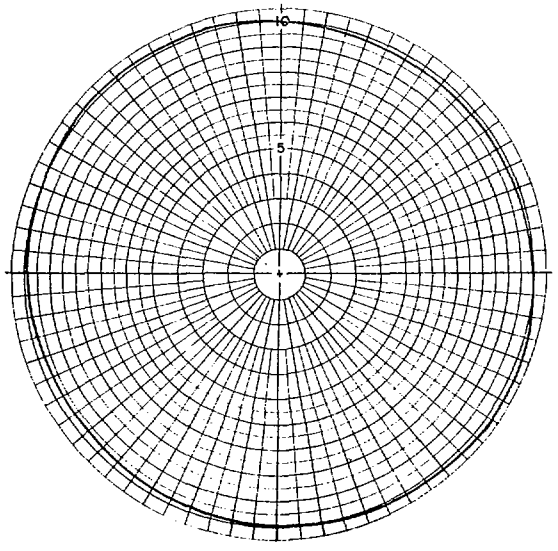


Fig. 11—Polarization pattern for 40-turn, 13° helix; $f=8$ kmc.

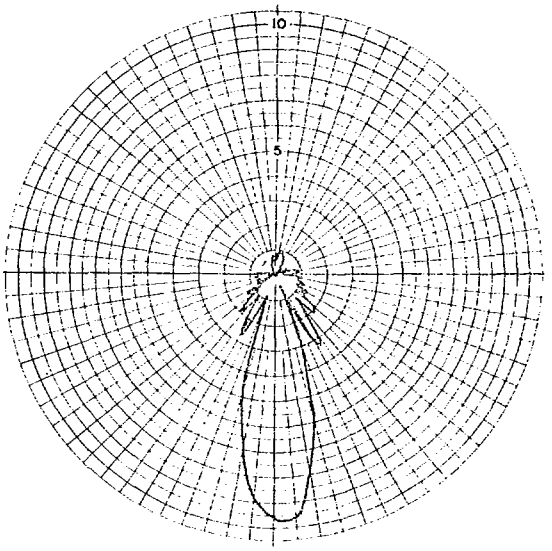


Fig. 12—$E_\theta$ pattern for 30-turn, 13° helix; $f=8$ kmc.

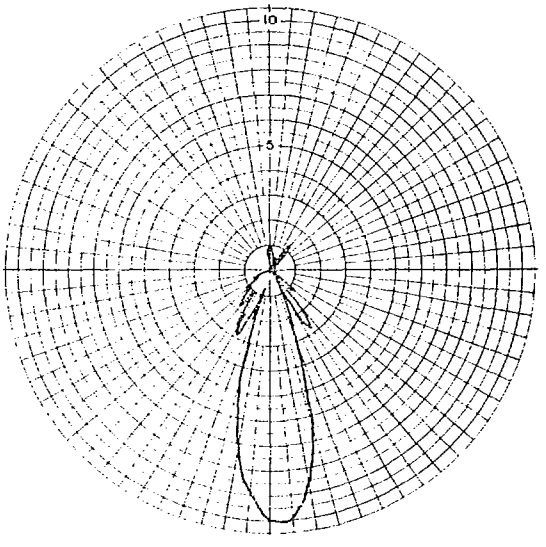


Fig. 13—$E_\phi$ pattern for 30-turn, 13° helix; $f=8$ kmc.

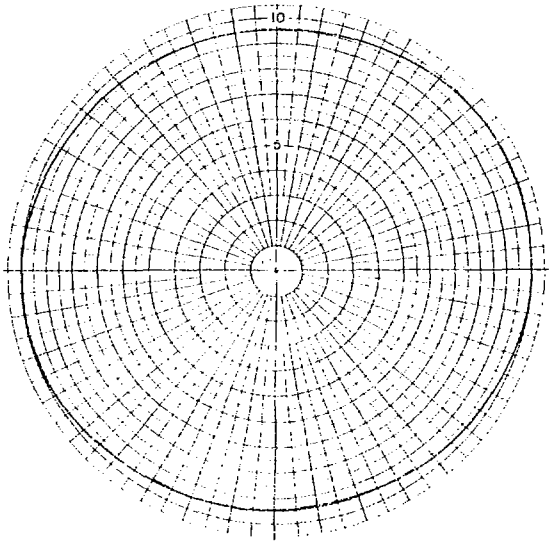


Fig. 14—Polarization pattern for 30-turn, 13° helix; $f=8$ kmc.

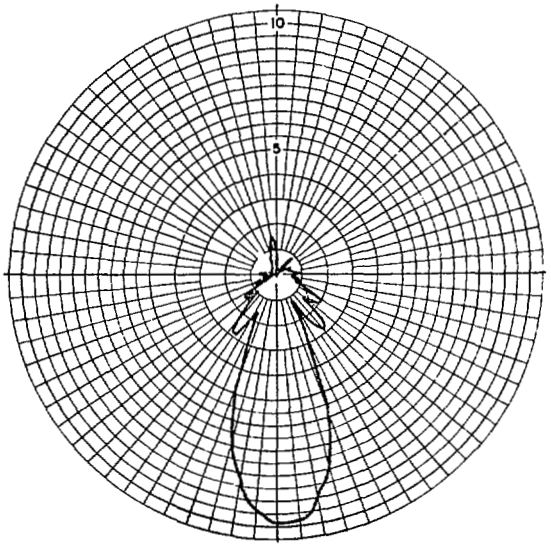


Fig. 15—$E_\theta$ pattern for 20-turn, 13° helix; $f=8$ kmc.

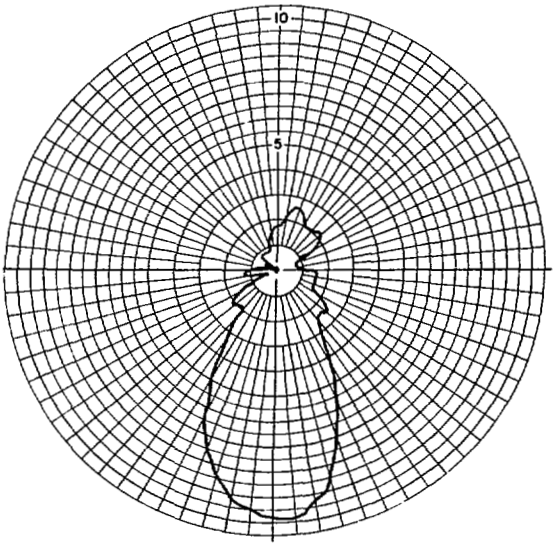


Fig. 18—$E_\theta$ pattern for 10-turn, 13° helix; $f=8$ kmc.

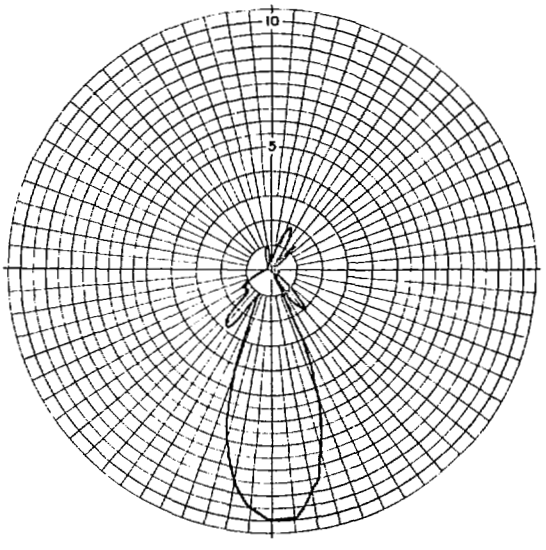


Fig. 16—$E_\phi$ pattern for 20-turn, 13° helix; $f=8$ kmc.

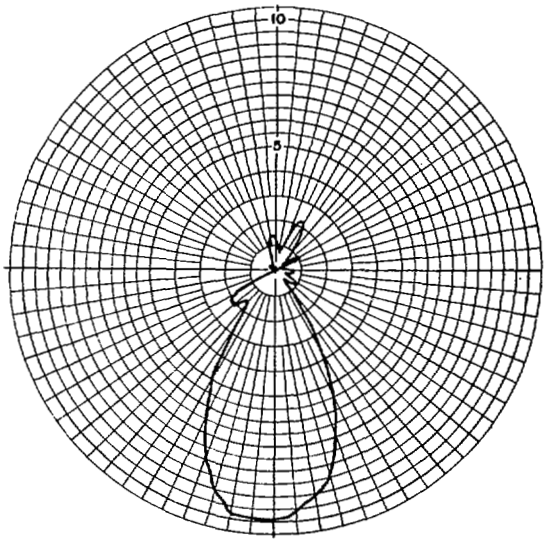


Fig. 19—$E_\phi$ pattern for 10-turn, 13° helix; $f=8$ kmc.

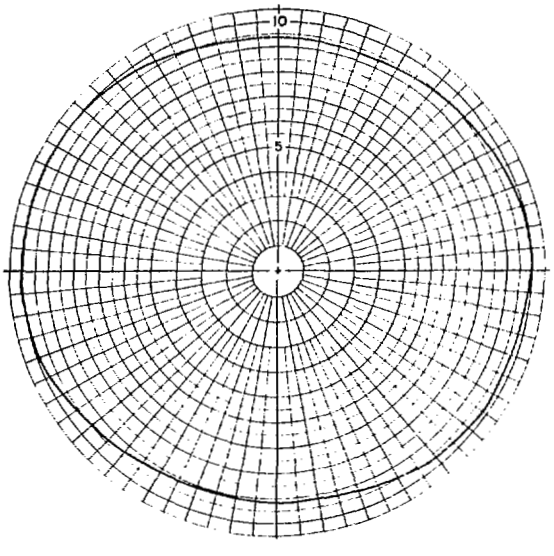


Fig. 17—Polarization pattern for 20-turn, 13° helix; $f=8$ kmc.

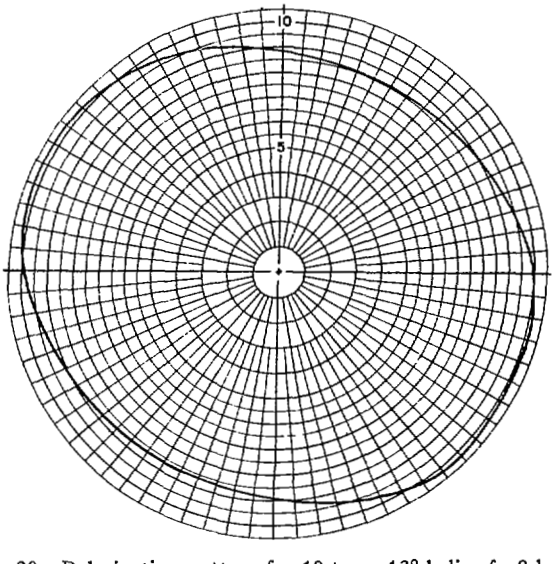


Fig. 20—Polarization pattern for 10-turn, 13° helix; $f=8$ kmc.

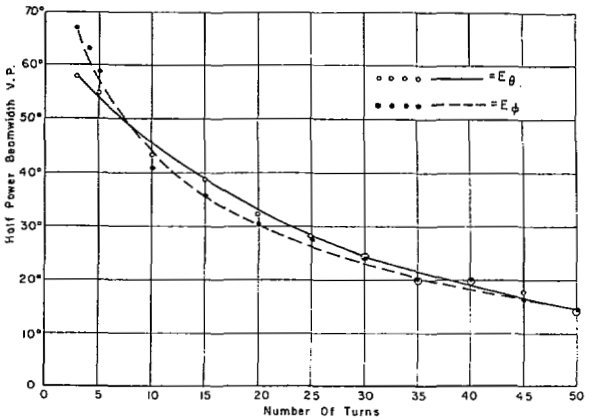


Fig. 21—Half-power beamwidth vs number of turns, $f=8$ kmc, 13° helix.

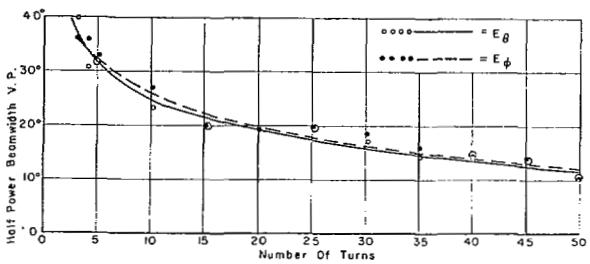


Fig. 22—Minimum half-power beamwidth vs number of turns, 13° helix.

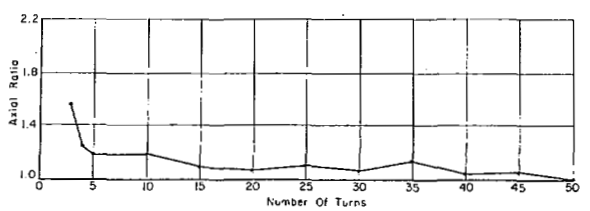


Fig. 23—Voltage axial ratio vs number of turns, 13° helix; $f=8$ kmc.

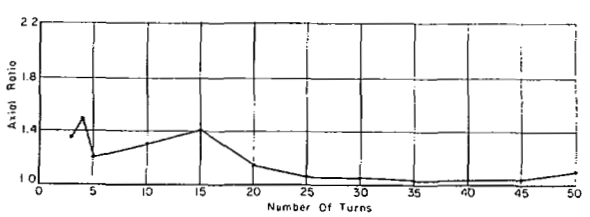


Fig. 24—Voltage axial ratio vs number of turns, 13° helix; at upper frequency limits.

## Approximate Graphical Solution to Determinantal Equation for Medium-Pitch Helix $\psi=13°$

The solution to the determinantal equation for the infinite helix with $\psi=13°$ has been given as curve (a) in Figs. 3 and 4. An alternative way of presenting the same information is to show the solution on the same graph as the pass band region, as illustrated in Fig. 25. This has an advantage in that it shows clearly the degree of approximation in an approximate graphical solution suggested by Sensiper,[2] which takes the form of the two straight lines $AB$ and $BC$. $AB$ lies along the edge of the forbidden region $m=-1$, and $BC$ is that portion of the

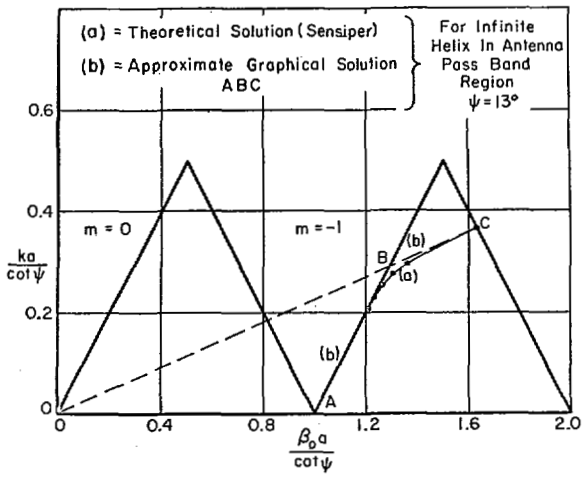


Fig. 25—Solutions of determinantal equation for $\psi=13°$.

line $ka/\cot\psi=|\beta_0|a/\cot\psi\cdot\sin\psi$ that lies between the $m=-1$ and $m=-2$ forbidden regions.

It will be seen that the approximate graphical solution always gives a value of phase velocity along the axis of the antenna which is too high. Nevertheless, in the medium-pitch angle range it offers a quick method of estimating the upper frequency limit along $BC$, the solution obtained being about 15 per cent above the exact solution for long helices. It should be mentioned, perhaps, that this approximation involves only a few minutes work compared with the several days of computation required for the exact solution.

## The Bandwidth of a Narrow-Pitch Helix

An examination of the narrow-pitch helix was begun after the approximate graphical solution to the determinantal equation had indicated that propagation of the axial-beam mode with the proper phase velocity appeared to be possible even for narrow-pitch helices. It was further believed that the existence of this mode if, in fact, it did propagate, might have been overlooked in the past because of concentration on the center frequency of $C_\lambda=1$. The advantage of applying Sensiper's theory in this case is that it indicates that the first experimental check for the mode should be made in the vicinity of the lower frequency limit which is well below $C_\lambda=1$.

An experimental model was constructed with the smallest pitch angle which could be wound with enamelled wire of diameter 0.032 inch, at 3-cm wavelength —this was an angle of 1.8°. At this pitch angle, the turns were in physical contact and the helix, of length about 1.5 λ, was self-supporting. No success was achieved with this model, and it was therefore decided to construct a longer one of length 4 λ, wound with 181 turns. This was found to give good patterns and a good axial ratio, having an upper frequency limit of 0.81 $C_\lambda$ compared with 1.1 $C_\lambda$ for the 13° pitch helix. Three of the patterns obtained are shown in Figs. 26–28.

The propagation constant for this helix was solved

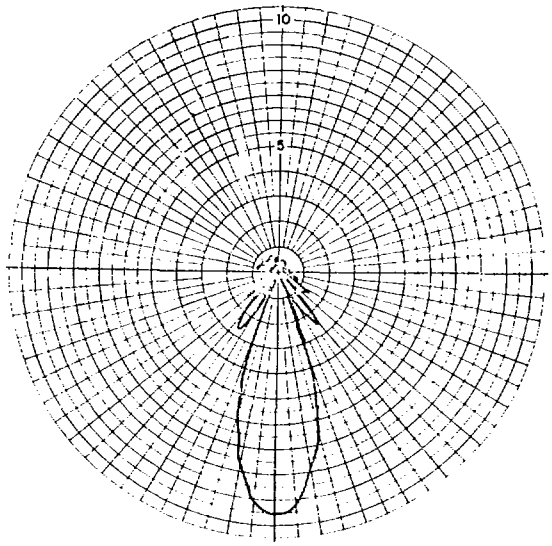


Fig. 26—$E_\theta$ pattern for 181-turn, 1.8° helix; $f=8$ kmc.

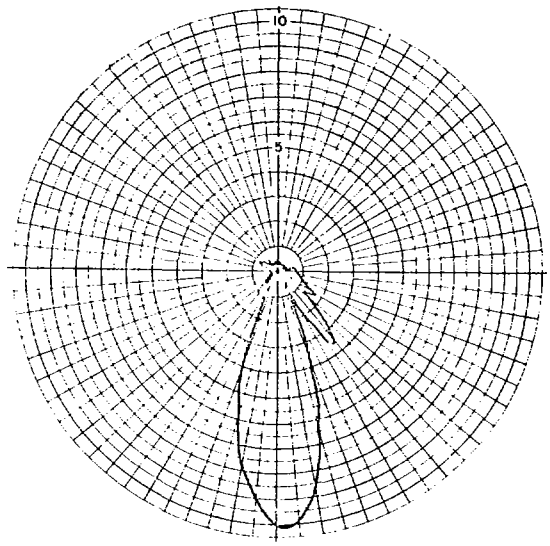


Fig. 27—$E_\phi$ pattern for 181-turn, 1.8° helix; $f=8$ kmc.

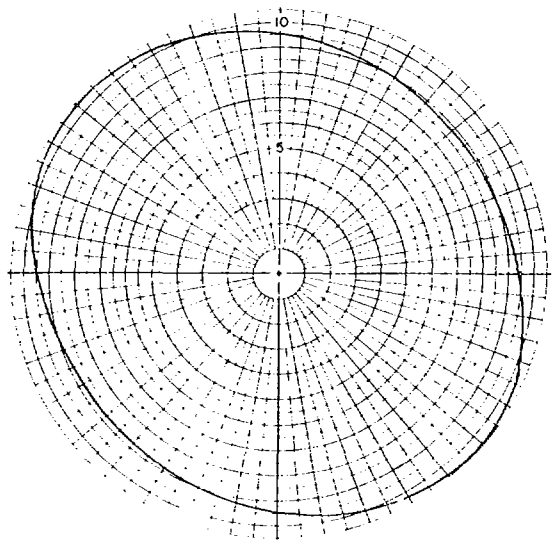


Fig. 28—Polarization pattern for 181-turn, 1.8° helix; $f=8$ kmc.

as in the medium-pitch case. One minor difference which should be noted is that asymptotic expressions for the modified Bessel functions must be used since the arguments of interest are outside the range of tabulated values. It was found that the upper frequency limit for the same criterion of sidelobe level as in the medium-pitch case was $0.87\ C_\lambda$. The argeement with experimental results is therefore of the same order as for $\psi=13°$.

An additional antenna with the same pitch angle and of length $2\ \lambda$ was constructed and was found to give less satisfactory patterns, although it still satisfied the condition for increased directivity. It appears that it may be more difficult to excite the surface wave on a short narrow-pitch helix than on a medium-pitch helix of the same length. This may be because the axial phase velocity is less for $\psi=1.8°$ than for $\psi=13°$, so that a greater length of helix is necessary to bring about this reduction of velocity. Some evidence exists which suggests that the necessary over-all length may be reduced by starting off the helix winding with a medium-pitch turn before proceeding to the remainder of narrow-pitch. This will be discussed further in a separate report on the modulated helix.

No claim that the narrow-pitch-angle helix is superior to the medium-pitch helix in radiation pattern seems to be proper, nor is it expected that there will be any advantage in impedance characteristics. It is relevant to suggest, however, that for a constant length and constant diameter, there must be at least some difference in the axial phase velocity since it seems reasonable to presume that the different conductor dispositions result in different dielectric constants for the artificial dielectric medium. It would appear from past experiments that this effect is relatively small.

The elimination of this gap in the lower pitch-angle range is satisfying since, from a theoretical viewpoint, there is no valid reason for it to exist. It is now believed that a satisfactory pattern may be obtained for any pitch angle up to the value where the deterioration is caused by the pattern of the array factor.

## Conclusions

It has been shown that the propagation constant determined from the theoretical solution for propagation along an infinite helix can be used to predict the upper frequency limit of a finite helical antenna of medium pitch angle, and of any length up to about ten wavelengths with an accuracy of the order of ten per cent.

This upper frequency limit decreases considerably with length, *e.g.*, from 1.35 $C_\lambda$ for a three-turn helix down to 1.0 $C_\lambda$ for a 50-turn helix. The patterns in this range always satisfy the increased directivity condition, and the voltage axial ratios are less than 1.2 from 5 to 50 turns.

It has been established that radiation in the beam mode with good patterns and axial ratio can be obtained from a helical antenna four wavelengths long with a pitch angle as low as 1.8°.